Imaginal Discs Secrete Insulin-Like Peptide 8 to Mediate Plasticity of Growth and Maturation

Andres Garelli *et al.*

Science **336**, 579 (2012);
DOI: 10.1126/science.1216735

Imaginal Discs Secrete Insulin-Like Peptide 8 to Mediate Plasticity of Growth and Maturation

Andres Garelli,* Alisson M. Gontijo,* Veronica Miguela, Esther Caparros, Maria Dominguez†

Developing animals frequently adjust their growth programs and/or their maturation or metamorphosis to compensate for growth disturbances (such as injury or tumor) and ensure normal adult size. Such plasticity entails tissue and organ communication to preserve their proportions and symmetry. Here, we show that imaginal discs autonomously activate DILP8, a *Drosophila* insulin-like peptide, to communicate abnormal growth and postpone maturation. DILP8 delays metamorphosis by inhibiting ecdysone biosynthesis, slowing growth in the imaginal discs, and generating normal-sized animals. Loss of *dilp8* yields asymmetric individuals with an unusually large variation in size and a more varied time of maturation. Thus, DILP8 is a fundamental element of the hitherto ill-defined machinery governing the plasticity that ensures developmental stability and robustness.

Animal size is remarkably constant within species. This constancy is even more striking within the animal, such as in comparing the left and right sides of bilaterian organisms—for example, the symmetry of a human face or the coincidence in size of the left and right hand. Such precision requires growing organs to communicate and coordinate their final sizes, processes that have long remained poorly understood (*1*).

The imaginal disc epithelia that generate the adult *Drosophila* structures have a remarkable capacity to regulate their size, although only in larvae (*2*). The onset of the larval-pupal transition is controlled by pulses of the steroid hormone 20-hydroxyecdysone (20HE), as initiated by brain-derived prothoracicotropic hormone (PTTH), and this transition marks the end of imaginal disc growth (*3*, *4*). Typically, the time of pupariation adapts to accommodate imaginal disc growth (*4*), and indeed, pupariation is delayed when imaginal discs suffer lesions to allow the missing parts to be restituted (*5*–*7*). The length of the delay correlates with the amount of tissue to be regenerated (*6*), indicating that the endocrine system fine-tunes organ growth (or regeneration) and adjusts maturation accordingly. Tumor growth in imaginal discs also delays or blocks metamorphosis [(*8*) and citations therein]. Moreover, larvae with imaginal discs that are damaged or contain tumors metamorphose at the correct size (*9*). Thus, we speculated that tumors and regenerating discs might emit a common signal to adapt growth and maturation.

We attempted to identify such a signal in oligonucleotide microarrays (fig. S1) by screening for genes encoding signal peptides that are up-regulated in association with tumors in eye discs induced by an oncogenic combination of the Notch ligand *Delta* and two neighboring epigenetic repressors, *pipsqueak* and what are collectively called "eyeful" (*10*), which causes massive overgrowth and metastasis. *CG14059* was the most consistently enriched putatively secreted gene product in tumor discs (Fig. 1A and table S1) and was also enriched during transdetermination (*11*),

Instituto de Neurociencias, Consejo Superior de Investigaciones Científicas–Universidad Miguel Hernández de Elche, Sant Joan d'Alacant, 03550 Alicante, Spain.

*These authors contributed equally to this work.
†To whom correspondence should be addressed. E-mail: m.dominguez@umh.es

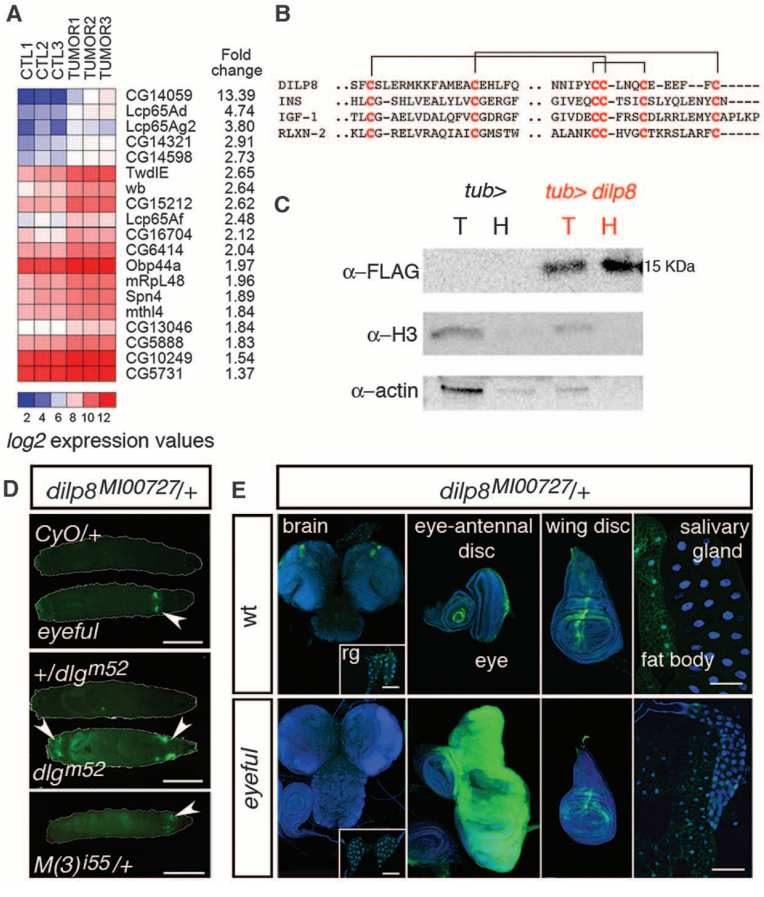

Fig. 1. Tumor discs produce DILP8, a divergent insulin/relaxin-like peptide. (**A**) Heat map of putatively secreted genes up-regulated in eyeful tumor eye discs from three independent replicates (1 to 3) of microarray experiments in which expression is color-coded. Relative gene expression levels are color-coded to range from blue (lower levels of gene expression), through white (medium expression), to red (higher levels of expression). CTL, control non-tumor eye discs [+/*UAS-Dl GS(2)88A8*$^{lola\ pipsqueak}$]; TUMOR, eyeful tumor eye discs [+/*ey-Gal4 UAS-Dl GS(2)88A8*$^{lola\ pipsqueak}$]. (**B**) Alignments of CG14059/DILP8 with representative members of the human insulin-like family of peptides. Alignments of DILP8 with the seven *Drosophila* ILPs characterized previously are shown in fig. S1. (**C**) DILP8 is readily detected in the cell-free hemolymph (H) of *tub>dilp8::3x-FLAG* larvae in Western blots probed with anti-FLAG antibodies. Total (T) hemolymph extract serve as loading controls. Samples are free of cell contamination, as shown by actin and histone H3 controls. (**D**) Responses of eGFP trap *dilp8*^{MI00727} to abnormal imaginal disc growth (arrowheads). Scale bars, 1 mm. Controls (top images in top two panels) are sibling larvae that were either CyO/+ (wild type; top) or heterozygous +/*dlg*^{m52} (middle). Representative heterozygous third chromosome Minute mutant, M(3)^{i55}, is shown at bottom. (**E**) Confocal images show GFP (green) and 4′,6-diamidino-2-phenylindole (DAPI) (blue) staining in wild type (top) and eyeful (bottom) larvae heterozygous for *dilp8*^{MI00727}. Brain expression is delayed in the eyeful tumor model. rg, ring gland.

another process that delays pupariation. Because the gene product had an invariant 6-cysteine motif typical of the insulin-relaxin peptide family (Fig. 1B and figs. S1 and S2), we named this gene *Drosophila* insulin-like peptide 8 (*dilp8*). This is the only DILP differentially expressed in tumors (fig. S3). The secretion of DILP8 was confirmed by expressing a carboxy-terminal FLAG-tagged construct, which, consistent with its hormonal nature, was detected in larval hemolymph (Fig. 1C) and in the medium of transfected Schneider (S2) cells (fig. S4).

We examined the native and induced expression of *dilp8* using an enhanced green fluorescent protein (eGFP) trap in the gene's first intron [*Mi{MIC}CG14059*^{MI00727} (*12*), hereafter *dilp8*^{MI00727} (fig. S5)]. Larval eGFP expression was assessed in mutants with different growth perturbations in the imaginal discs that delay pupariation: fast-growing tumors induced by oncogene activation (*10*); slow-growing tumors, exemplified by a recessive mutation in the tumor-suppressor gene *discs large* [*dlg*^{m52} (*13*)]; and slow growth of imaginal discs due to *Minute* mutations (*9*). In all cases, there was cell-autonomous induction of eGFP in the affected third-instar imaginal discs (Fig. 1, D and E, and fig. S6), as well as weak and dynamic signals in the normally growing discs and brain (Fig. 1E). Hence, DILP8 is a common response to abnormal imaginal disc growth, and the response is conserved in other *Drosophila spp.* (fig. S7).

Using the homozygous *dilp8*^{MI00727} insertional mutation that reduces *dilp8* mRNA expression by 99.4% (Fig. 2A), we investigated whether *dilp8* influences pupariation. In synchronous larvae, loss of *dilp8* reverted the delay in pupariation caused by eye disc tumors from 26.6 ± 7.5 hours to 5.9 ± 7.1 hours (mean ± SD pupariation time, $P = 0.026$) (Fig. 2B).

To determine whether the *dilp8* response is tumor-selective or broadly used, we assayed

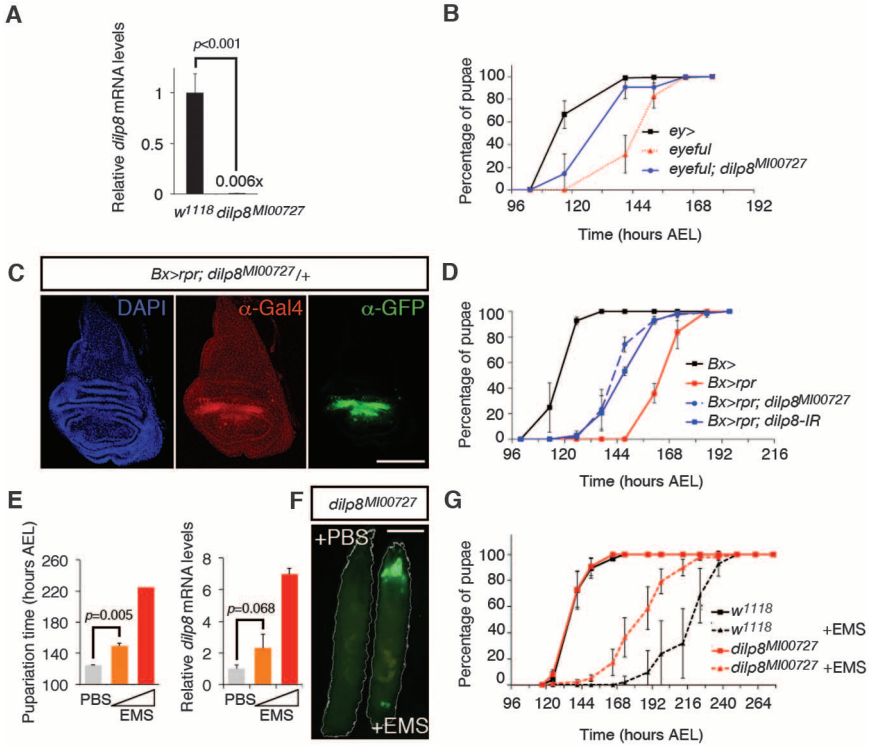

Fig. 2. DILP8 is required for adaptive developmental plasticity in imaginal discs growing abnormally. (**A**) *dilp8* expression relative to *rp49* analyzed by means of quantitative reverse transcription polymerase chain reaction (RT-PCR) in virgin females of the wild type (*w*^{1118}) or homozygous *dilp8*^{MI00727} mutant (mean ± SD of three or four independent replicates) (fig. S5). (**B**) Loss of *dilp8* in the eyeful tumor background rescues delayed pupariation. Three replicates were scored, each with two to five tubes containing ~30 larvae. (**C**) Confocal images of GFP (green) and GAL4 (red) staining in *Bx>rpr;dilp8*$^{MI00727/+}$ wing discs (DAPI, blue). Scale bar, 100 μm. (**D**) Depletion of *dilp8* in *Bx>rpr* animals partially rescues the delay in pupariation ($n = 5$ replicates of two to five tubes of ~25 larvae per genotype scored). (**E**) Pupariation time and *dilp8* expression analyzed by means of quantitative RT-PCR in animals fed with phosphate-buffered saline or two doses of EMS (10 to 20 mM). (**F**) EMS (10 mM) activated the eGFP reporter in damaged discs. Scale bar, 1 mm. (**G**) *dilp8*^{MI00727} reduced the delay in pupariation in EMS-fed larvae (four tubes of ~25 larvae were scored per genotype and treatment). *ey>* and *Bx>* indicate *eyeless (ey)-Gal4/+* and *P{GawB}Bx*^{MS109}*/+* and serve as genetic background controls.

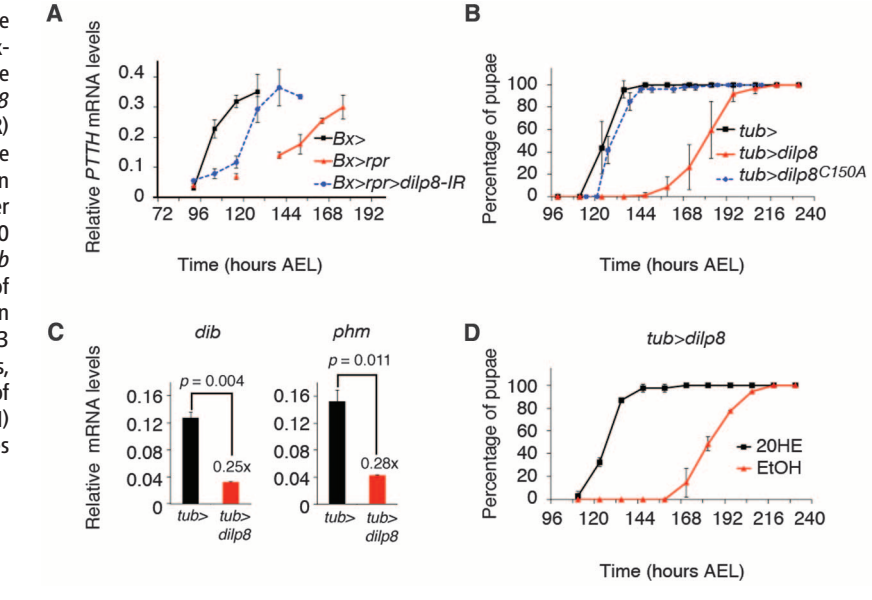

Fig. 3. DILP8 delays metamorphosis by regulating the expression of ecdysone biosynthetic genes. (**A**) PTTH expression relative to *rp49* analyzed by means of quantitative RT-PCR in synchronous *Bx>rpr* larvae with or without *dilp8* RNAi silencing induced by expression of inverted repeat (IR) transgene. The mRNA was isolated from approximately five larvae per time point and genotype. (**B**) *dilp8* overexpression delayed pupariation ($n = 3$ to 4 tubes of ~20 larvae each per genotype). The cysteine-to-alanine mutation at residue 150 (C150A) renders a biologically inactive DILP8 protein. (**C**) *dib* (left) and *phm* (right) expression analyzed by means of quantitative RT-PCR in mRNA isolated from ring gland/brain complexes from synchronous larvae (118 hours AEL; $n = 3$ replicates, each with RNA isolated from ~20 ring gland/brains, mean ± SD two-tailed unpaired *t* test). (**D**) Pupariation time of *tub>dilp8* larvae fed 20HE (0.5 mg/mL) or the ethanol (EtOH) as vehicle ($n > 40$ larvae per treatment). *tub>* indicates *tubulin-Gal4/+* and serves as background control.

dilp8 expression and activity during regeneration induced by two forms of damage. First, cell death was induced by overexpressing the proapoptotic gene *reaper* (*rpr*) by using *Beadex-Gal4* (*Bx>rpr*), which provokes continuous intrinsic damage and regenerative growth in the wing pouch, and a pupariation delay (*14*). *dilp8* transcripts were up-regulated in third-instar *Bx>rpr* larvae (fig. S8), and the $dilp8^{MI00727}$ reporter was activated cell-autonomously in damaged/regenerating cells (Fig. 2C and fig. S8). When *dilp8* was diminished in whole *Bx>rpr* larvae by $dilp8^{MI00727}$ mutation or by tissue-specifically reducing *dilp8* mRNA by 71% through RNA interference (RNAi) (*Bx>rpr>dilp8-IR*) (fig. S9), the delay in pupariation reverted from 46.2 ± 1.3 hours to 27.8 ± 2.9 hours ($P < 0.001$) and 29.1 ± 2.5 hours ($P < 0.001$), respectively (Fig. 2D).

Secondly, synchronized larvae were fed with the genotoxic agent ethyl methanosulfonate (EMS) administered from 72 hours after egg-laying (AEL), which produced a dose-dependent delay in pupariation (Fig. 2E), strong caspase activation in imaginal discs, yet only mild defects in adult structures (fig. S10), which is similar to that caused by DNA damage and repair following irradiation (*14*, *15*). In imaginal discs of $dilp8^{MI00727}$ larvae, eGFP highlighted the damage produced by EMS (Fig. 2F), and this response of *dilp8* was dose-dependent (Fig. 2E), indicating that *dilp8* is tightly associated with the extent of damage/regeneration. The endogenous $dilp8^{MI00727}$ mutation shortened the delay induced by EMS by 44.03% ± 13.24 ($P <$ 0.0001) (Fig. 2G), and *dilp8* RNAi (*tub>dilp8-IR*) reduced this delay by 43.24% ± 9.36 ($P = 0.0063$) (fig. S11). Moreover, *dilp8* depletion augmented the pupal lethality associated with exposure to EMS (fig. S11). Thus, DILP8 regulates the timing of pupariation in response to tumor and regenerative growth and increases survival after tissue insult.

We examined the expression of hormone genes regulating the larval-to-pupal transition in relation to DILP8. Cell death–induced damage by *Bx>rpr* delays metamorphosis inhibiting PTTH synthesis in the brain, a delay that is enhanced by the consumption of provitamin A (ß-carotenoids) in the diet (*14*). Down-regulating *dilp8* attenuated the PTTH delay by some 12 to 24 hours (Fig. 3A), independently of retinoids (fig. S12), indicating that DILP8 is required to delay PTTH synthesis in damaged/regenerating tissues.

We next assessed whether DILP8 is sufficient to delay pupariation in the absence of growth abnormalities. Synchronized larvae overexpressing *dilp8* driven by *tub-Gal4* (*tub>dilp8*) initiated pupariation 55.9 ± 7.6 hours later than did control *tub>* or $tub>dilp8^{C150A}$ larvae that overexpress *dilp8* mutated at a conserved cysteine ($P < 0.001$) (Fig. 3B). Compared with the damaged *Bx>rpr* animals, *dilp8* overexpression caused delayed induction of transcription of the *disembodied* (*dib*) and *phantom* (*phm*) genes in the ecdysone synthesis cascade (Fig. 3C and fig. S13) without delaying PTTH (fig. S13). The delay in pupariation induced by DILP8 was overcome by feeding larvae 20HE (Fig. 3D), confirming that the effects of DILP8 were a consequence of reduced ecdysone production.

Damaged and regenerating larvae, or those with tumor discs, attain a wild-type size. Similarly, although *tub>dilp8* larvae prolong their feeding (longer than the controls), they were no larger (Fig. 4A and fig. S14). However, this extended feeding made *tub>dilp8* adults weigh more than controls (Fig. 4B and fig. S15).

To attain correct final size despite their prolonged larval life span, DILP8 overexpression may also exert control on growth rates to prevent overgrowth. Hence, we quantified the transcription of *Thor* (*d4E-BP*), a direct target of the growth inhibitor FOXO, as surrogate measure for imaginal disc growth (*16*–*18*). *Thor* expression was selectively up-regulated in *tub>dilp8* imaginal discs (Fig. 4C), which is consistent with a slower imaginal disc growth. In contrast, *Thor* expression in the fat body (fig. S15) showed that insulin/insulin-like growth factor 1 (IGF-1) signaling was not generally impaired, as also evident through the analysis of *dilp2* and *dilp3* expression (fig. S16). Thus, DILP8 exerts a fundamental influence on an adaptive plasticity of both growth and maturation, either directly or via secondary signals.

In the absence of such plasticity, organisms would be incapable of adjusting the growth of distinct body parts to maintain their overall proportionality and left-right symmetry. Indeed, $dilp8^{MI00727}$ animals pupate over an extended time scale and are more varied in size than controls sharing the same genetic background

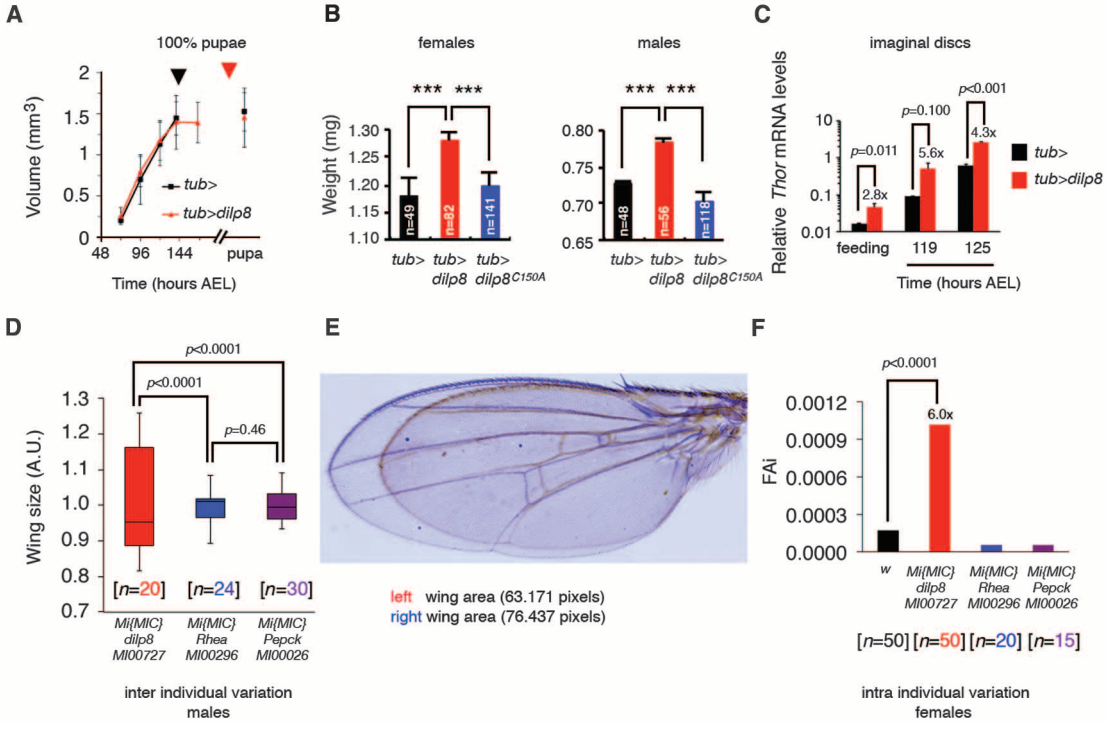

Fig. 4. DILP8 reduces inter- and intra-individual phenotypic variations, reflecting greater developmental stability and robustness. (**A**) Growth rate curve derived by scoring >10 animals of each genotype and time point. Multiple pair-wise two-tailed unpaired *t* tests with Bonferroni correction showed no significant differences ($P > 0.10$). Arrowheads indicate the time of 100% pupation for each genotype. (**B**) Virgin female and male adults overexpressing *dilp8* weigh more than controls (***$P < 0.001$, mean ± SD two-tailed unpaired *t* test with Bonferroni correction), although their overall size is the same (fig. S14). (**C**) *Thor* expression in imaginal discs from synchronous *tub>* or *tub>dilp8* third-instar larvae relative to *rp49* and *dUba2*, analyzed by means of quantitative RT-PCR (feeding larvae, ~115 hours AEL, $n = 3$ biological replicates, each with RNA isolated from imaginal discs of ~20 larvae per genotype, mean ± SD two-tailed unpaired *t* test). (**D**) Box-and-whiskers plot of the wing area of $dilp8^{MI00727}$ and control of genetic background ($Rhea^{MI00296}$ and $Pepck^{MI00026}$) males ($P < 0.0001$, *f* test for unequal distributions). The three Mi{MIC} insertions were generated in the same genetic background (*12*). (**E**) Comparisons of the left and right wings of a $dilp8^{MI00727}$ female. (**F**) Bar graphs of the FAi of the left and right wings of the genotypes indicated (*20*). Numbers in brackets in (D) and (F) are the wing pairs scored.

(Fig. 4D and fig. S17). Individually, *dilp8*^{MI00727} flies reared at 26.5°C display imperfect bilateral symmetry (Fig. 4E), and when intra-individual variation between the left and right wings was assessed by using the fluctuating asymmetry index (FAi) (*19*, *20*), wing FAi was statistically significantly higher in *dilp8*^{MI00727} females than in w^{1118} (Fig. 4F). This higher asymmetry reflects lesser stability (*19*).

Collectively, our results suggest that DILP8—an insulin/IGF/relaxin–like hormone peptide (Fig. 1)—provides a signal that communicates the growth status of peripheral tissues in order to regulate developmental timing, population robustness, and individual developmental stability [detected by fluctuating asymmetry analysis (*19*)], as well as local responses to processes such as regeneration and cancer.

References and Notes

1. H. F. Nijhout, *Dev Biol* **261**, 1 (2003).
2. P. J. Bryant, O. Schmidt, *J. Cell Sci. Suppl.* **13**, 169 (1990).
3. J. M. Tennessen, C. S. Thummel, *Curr. Biol.* **21**, R750 (2011).
4. A. W. Shingleton, *Organogenesis* **6**, 76 (2010).
5. C. A. Poodry, D. F. Woods, *Rouxs Arch. Dev. Biol.* **199**, 219 (1990).
6. P. Simpson, P. Berreur, J. Berreur-Bonnenfant, *J. Embryol. Exp. Morphol.* **57**, 155 (1980).
7. R. K. Smith-Bolton, M. I. Worley, H. Kanda, I. K. Hariharan, *Dev. Cell* **16**, 797 (2009).
8. L. Menut *et al.*, *Genetics* **177**, 1667 (2007).
9. B. C. Stieper, M. Kupershtok, M. V. Driscoll, A. W. Shingleton, *Dev. Biol.* **321**, 18 (2008).
10. D. Ferres-Marco *et al.*, *Nature* **439**, 430 (2006).
11. A. Klebes *et al.*, *Development* **132**, 3753 (2005).
12. K. J. Venken *et al.*, *Nat. Methods* **8**, 737 (2011).
13. D. F. Woods, P. J. Bryant, *Dev. Biol.* **134**, 222 (1989).
14. A. Halme, M. Cheng, I. K. Hariharan, *Curr. Biol.* **20**, 458 (2010).
15. L. A. Abbott, *Radiat. Res.* **96**, 611 (1983).
16. M. A. Jünger *et al.*, *J. Biol.* **2**, 20 (2003).
17. M. Miron *et al.*, *Nat. Cell Biol.* **3**, 596 (2001).
18. V. Hietakangas, S. M. Cohen, *Annu. Rev. Genet.* **43**, 389 (2009).
19. A. R. Palmer, C. Strobeck, *Annu. Rev. Ecol. Syst.* **17**, 391 (1986).
20. Materials and methods are available as supplementary materials on *Science* Online.

Acknowledgments: We thank E. Hafen, L. Garcia-Alonso, B. Lakowski, and F. Heredia for their comments and suggestions; J. Colombani, D. S. Andersen, and P. Léopold for sharing unpublished data; and I. Gutierrez and E. Ballesta for technical help. V.M. is a Generalitat Valenciana fellow, and A.M.G. was supported by a Marie Curie Fellowship. This work was supported by grants from the Fundación Botin, the Ministerio de Ciencia e Innovación (BFU2009-09074 and MEC-CONSOLIDER/CSD2007-00023), Generalitat Valenciana (PROMETEO/2008/134), and the European Commission (HEALTH-F2-2008-201666) to M.D. The microarray data are deposited in the Gene Expression Omnibus (GEO) repository (accession GSE35471). A.M.G. and M.D. designed the research; A.G., A.M.G., V.M., E.C., and M.D. performed the experiments and analyzed the data. A.G., A.M.G., and M.D. wrote the manuscript.

Supplementary Materials

www.sciencemag.org/cgi/content/full/336/6081/579/DC1
Materials and Methods
Figs. S1 to S17
Table S1
References (*21*–*27*)

16 November 2011; accepted 30 March 2012
10.1126/science.1216735

Secreted Peptide Dilp8 Coordinates *Drosophila* Tissue Growth with Developmental Timing

Julien Colombani,* Ditte S. Andersen,*† Pierre Léopold†

Little is known about how organ growth is monitored and coordinated with the developmental timing in complex organisms. In insects, impairment of larval tissue growth delays growth and morphogenesis, revealing a coupling mechanism. We carried out a genetic screen in *Drosophila* to identify molecules expressed by growing tissues participating in this coupling and identified *dilp8* as a gene whose silencing rescues the developmental delay induced by abnormally growing tissues. *dilp8* is highly induced in conditions where growth impairment produces a developmental delay. *dilp8* encodes a peptide for which expression and secretion are sufficient to delay metamorphosis without affecting tissue integrity. We propose that Dilp8 peptide is a secreted signal that coordinates the growth status of tissues with developmental timing.

Classical regeneration experiments in insects have demonstrated an important role for imaginal tissues (also called "discs," the larval tissues that give rise to the adult appendages) in coupling tissue growth, maturation, and patterning during development (*1*). When disc growth is impaired, the duration of the larval period is extended, allowing tissues to regenerate and/or grow to their target size before entering metamorphosis (*2*–*9*). However, when discs are strongly reduced or absent, larvae enter metamorphosis with normal timing (*5*). This suggests that discs that have not yet completed a certain amount of growth are able to inhibit the developmental transition leading to metamorphosis. We have used a genetic approach in *Drosophila* to identify signals emanating from growing larval discs that inhibit the onset of metamorphosis.

We first sought to identify conditions for which modification of disc growth would give rise to substantial developmental delay. We used the *rotund-Gal4* driver (*Rn>*) for disc-targeted RNA interference (RNAi) silencing of the *avalanche* gene (*avl*; *Rn>avl-RNAi*), encoding a syntaxin that functions in the early endocytic machinery (*10*), or the ribosomal protein L7-encoding gene (*rpl7*; *Rn>rpl7-RNAi*). Both conditions induced robust developmental delays of larva-to-pupa transition of about 2 to 3 and 3 to 5 days, respectively (Fig. 1A). *Rn>avl-RNAi* discs reach near -normal size after 5 days of development, then undergo unrestricted neoplastic growth (*10*) (Fig. 1, C to F). *Rn>rpl7-RNAi* animals grow at the same rate as control animals but fail to puariate at the normal time, giving rise to giant larvae and pupae after 2 to 3 days of extra growth (Fig. 1B and fig. S1E). In contrast, *Rn>rpl7-RNAi* discs grow and mature significantly slower than control discs and reach normal size after an extended period of growth (Fig. 1, C and G to I). Accordingly, *Rn>rpl7-RNAi* larvae grow at a slower rate and reach normal larvae and pupa sizes after an extended period of growth, as described for *Minute* mutants (Fig. 1B and fig. S1F) (*11*). In both conditions, the expression peaks of *phm* and *dib* [two genes involved in ecdysone biosynthesis (*12*)] were delayed (fig. S1, A and B), as was the activity peak of ecdysone (as measured by expression levels of its target gene, *E75B*) (fig. S1C) (*13*). The rise of expression of the prothoracicotropic hormone (PTTH) gene normally observed at the end of third larval instar was only slightly delayed (fig. S1D), indicating that *PTTH* expression is not limiting for pupariation in these conditions. Thus, in both conditions, altered disc growth acts upstream of ecdysone production to delay metamorphosis.

For our genome-wide approach, we used the *Rn>avl-RNAi* tester line to screen a collection of RNAi lines for their abilities to rescue the delay at pupariation (fig. S1G). Of the 10,100 lines tested, 121 significantly rescued the delay in *Rn>avl-RNAi* larvae. To eliminate candidates rescuing specifically the *Rn>avl-RNAi* condition, we rescreened the 121 lines by using the *Rn>rpl7-RNAi* tester line (fig. S1G). Of the 121 candidates, only one rescued both conditions efficiently (Fig. 1J). This RNAi line targets a previously uncharacterized gene, *CG14059*, which encodes a small peptide of about 150 amino acids, with a signal peptide followed by a cleavage site at its N terminus, and is therefore predicted to be secreted (fig. S5A). The peptide encoded by *CG14059* is characterized by a conserved code of cysteins found in many insulin-like peptides (*14*), and hence we called this gene *Drosophila insulin-like peptide 8* (*dilp8*). *dilp8* loss of function does not suppress the overgrowth phenotype observed in

Université de Nice, INSERM 1091, CNRS 7277, and France Institute of Biology, Parc Valrose, 06108 Nice, France.

*These authors contributed equally to this work.
†To whom correspondence should be addressed. E-mail: leopold@unice.fr (P.L.); andersen@unice.fr (D.S.A.)